CONFERENCE PRE-PRINT

IMPACT OF STARK BROADENING ON ION TEMPERATURE MEASUREMENTS IN THE ITER DIVERTOR PLASMA

M. GOTO
National Institute for Fusion Science
Toki, Japan
Email: goto.motoshi@nifs.ac.jp

K. NOJIRI
Naka Institute for Fusion Science and Technology, National Institutes for Quantum Science and Technology
Naka, Japan

A. CALISTI, S. FERRI, M. KOUBITI, J. ROSATO
Laboratoire PIIM, UMR 7345 Université d'Aix-Marseille/CNRS
Marseille, France

J. J. SIMONS
Graduate Institute for Advanced Studies, SOKENDAI
Toki, Japan

T. KAWATE
Naka Institute for Fusion Science and Technology, National Institutes for Quantum Science and Technology
Naka, Japan

T. OISHI
Department of Quantuim Science and Energy Engineering, Tohoku University
Sendai, Japan

E. YATSUKA
Naka Institute for Fusion Science and Technology, National Institutes for Quantum Science and Technology
Naka, Japan

Y. YANAGIHARA, M. ISOBE
National Institute for Fusion Science
Toki, Japan

Y. NUNOYA
Naka Institute for Fusion Science and Technology, National Institutes for Quantum Science and Technology
Naka, Japan

Abstract

The Stark broadening of the Be II line ($[1s^2]3d\,^2D - 4f\,^2F$, 467.339 nm) under a magnetic field is evaluated with the divertor plasma of ITER in mind. Electron and ion perturbers are treated in the impact and static approximations, respectively.

The perturbation term due to the magnetic field is included in the static approximation. The results show that the Stark broadening becomes significantly large when the density exceeds $5 \times 10^{20}\,\mathrm{m}^{-3}$, and the ion temperature would be overestimated if the Stark broadening is not taken into account. As alternative candidates, the B II lines ($[1s^2 2s]3d\ ^1D - 4f\ ^1F$, 412 nm and $[1s^2]2s2p\ ^1P - 2p^2\ ^1D$, 345 nm) are also examined. It is found that the 412 nm line is affected by Stark broadening when the density exceeds $5 \times 10^{20}\,\mathrm{m}^{-3}$, whereas the 345 nm line shows almost no influence. This indicates that simultaneous measurements of these emission lines could provide a means to evaluate both the ion temperature and the electron density.

1. INTRODUCTION

ITER's Divertor Impurity Monitor Diagnostic (DIM), consisting of several UV-visible spectrometers, is responsible for measuring the emission lines of impurity ions in the divertor region. One of the most important requirements of the DIM is the measurement of the ion temperature, T_i, in the divertor plasma. Since the ion temperature of the divertor is an important parameter affecting the sputtering of the divertor plates, a high precision measurement is required. On the other hand, the retention of impurity ions introduced into the divertor for radiation loss enhancement is the key challenge for efficient detachment sustainment, and it is also important to know the direction and magnitude of the impurity ion flow. For these reasons, the width, center wavelength, and intensity of the impurity ion emission lines must be accurately measured.

As coatings of low-Z materials such as beryllium or boron are considered for the divertor and the first wall plates in the current ITER design baseline, these impurity atoms and ions should be present in the divertor plasma and the T_i measurement can make use of the emission lines of these impurity ions. For accurate T_i measurements, it is necessary to clarify broadening effects on the emission line profile other than the Doppler broadening. First, there is an effect caused by magnetic fields. The magnetic field strength in the ITER plasma is typically 5 T, and the emission lines would split into several components due to the Zeeman effect. If the splitting width is comparable to the Doppler broadening width, the Zeeman effect could contribute to the observed broadening width.

Second, calculations with the SOLPS-ITER code [1] indicate that the electron density in the divertor plasma could exceed $10^{21}\,\mathrm{m}^{-3}$ near the target plates [2] where T_i is a few electron volts or less. Under such high density conditions, it is possible that the Stark broadening also affects the evaluation of the broadening width for the T_i measurement. We attempt to formulate a method for calculating the Stark broadening of impurity ion emission lines under a magnetic field.

We first evaluate the emission lines of beryllium ions, which have traditionally been considered as coating materials for the ITER vacuum vessel wall. However, due to recent policy changes at ITER that make the use of beryllium unlikely, we also present an evaluation of specific emission lines of boron ions, which are being considered for application in vacuum vessel wall conditioning.

2. CALCULATION METHOD OF STARK BROADENING UNDER MAGNETIC FIELD

The calculation follows Ref. [3], where electrons are treated in the impact approximation and ions in the static approximation. The ion microfields are described by the Holtsmark distribution [4,5] with the assumption $n_\mathrm{i} = n_\mathrm{e}$. The effect of a magnetic field $\boldsymbol{B}$ introduces axial symmetry, and the observable spectrum is obtained by convoluting the static- and impact-broadened profiles.

The Hamiltonian in combined $\boldsymbol{E}$ and $\boldsymbol{B}$ fields is

$$H = H_0 - \mu_\mathrm{B} B(g_L L_z + g_S S_z) - E d_\xi, \tag{1}$$

where d_ξ is the dipole operator along the $\boldsymbol{E}$ direction (See Fig. 1). The Zeeman term is evaluated by the usual method [6]. For the Stark term, basis states $|LJM\rangle$ must be rotated into the $\boldsymbol{E}$ direction,

$$|LJM\rangle = \sum_m |LJm\rangle_\xi D^{(J)*}_{Mm}(R), \tag{2}$$

using the Wigner rotation matrix $D^{(J)}_{Mm}(R)$ [7]. After diagonalizing Eq. (1), perturbed level energies and eigenvectors are obtained.

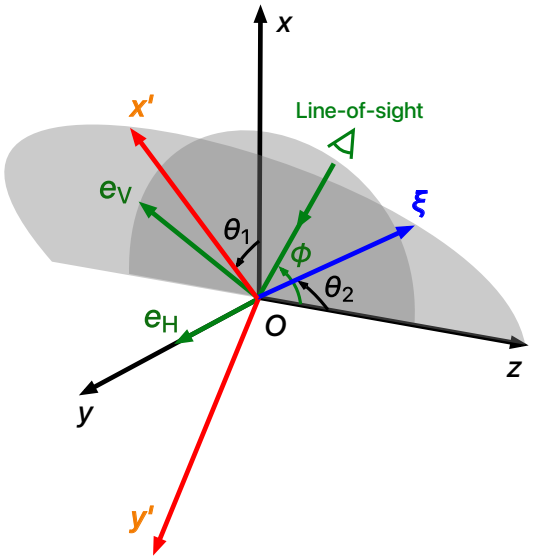

FIG. 1. Euler rotation for turning the quantization axis (z-axis) into the ξ-axis direction by first rotating θ_1 around the z-axis and then θ_2 around the y'-axis which is the new y-axis after the first rotation. The definition of observation vectors $\boldsymbol{e}_{\rm V}$ and $\boldsymbol{e}_{\rm V}$ are also shown: The former is in the x-z plane and is perpendicular to the line-of-sight, and the latter is on the y-axis.

The transition intensity is proportional to

$$I = |\langle l|\boldsymbol{e}\cdot\boldsymbol{d}|u\rangle|^2, \tag{3}$$

with $\boldsymbol{e}$ an observation vector. Two orthogonal vectors are taken: $\boldsymbol{e}_{\rm H}$ parallel to y, and $\boldsymbol{e}_{\rm V}$ in the x–z plane perpendicular to the line-of-sight (see Fig. 1). Dipole elements are expanded as

$$\langle l|d_q|u\rangle = \sum_{r,s} C_r^l C_s^u \langle L_1 J_1 M_1|d_q|L_2 J_2 M_2\rangle, \tag{4}$$

and evaluated by the Wigner–Eckart theorem and Racah algebra [9],

$$\begin{aligned}&\langle L_1 J_1 M_1|d_q|L_2 J_2 M_2\rangle \\ &= (-1)^{J_1-M_1}\begin{pmatrix} J_1 & 1 & J_2 \\ -M_1 & q & M_2\end{pmatrix}\begin{Bmatrix} L_1 & J_1 & S \\ J_2 & L_2 & 1\end{Bmatrix}\langle L_1||d||L_2\rangle.\end{aligned} \tag{5}$$

Finally, all magnetic sublevel combinations are summed, and integration over $\boldsymbol{E}$ with the Holtsmark distribution is carried out, followed by convolution with electron-impact broadening. This yields the line profile including Stark broadening in a magnetic field.

3. RESULTS AND DISCUSSION FOR BERYLLIUM ION LINE

For the impact approximation, the data found in Ref. [8] is adopted, where the line profile is approximated by the Lorentz function and is represented by the full width at half maximum (FWHM). The width is assumed to be proportional to the perturbers density, and its proportionality coefficient is given for respective lines. Figure 2 shows the spectra calculated for some different perturber density values. The thin lines show the spectra calculated with the method discussed in the previous section. The cross symbols show the convolution of the spectra with the Doppler broadening of 1 eV. Here, we give each data point a random error following the Poison distribution considering that fitting will be later performed with the Gaussian function to derive $T_{\rm i}$. It can been seen that the line is divided into three main peaks. The central peak and the two lateral peaks correspond to the π and σ components of the Zeeman split line, respectively. The intensity ratio of the π and σ components is mainly determined by the angle between the line-of-sight and the magnetic field, which is about 60 degrees.

Assuming a simple $T_{\rm i}$ measurement, the central peak is fitted with a single Gaussian, and $T_{\rm i}$ is determined from its width. Figure 3 shows the results for cases of $T_{\rm i} = 1$, 2, 5, 10, and 20 eV. It is readily noticed that the evaluated $T_{\rm i}$

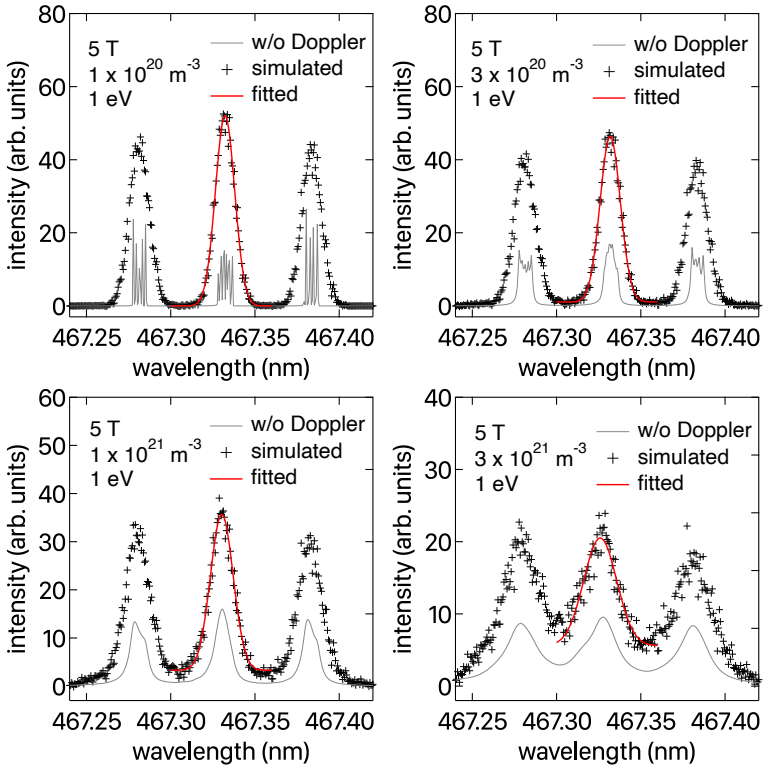

FIG. 2. Examples of calculated spectra of the Be II line ($1s^2 3d\ ^2D - 1s^2 4f\ ^2F$, 467.339 nm) for four different perturber density cases when $T_i = 1$ eV.

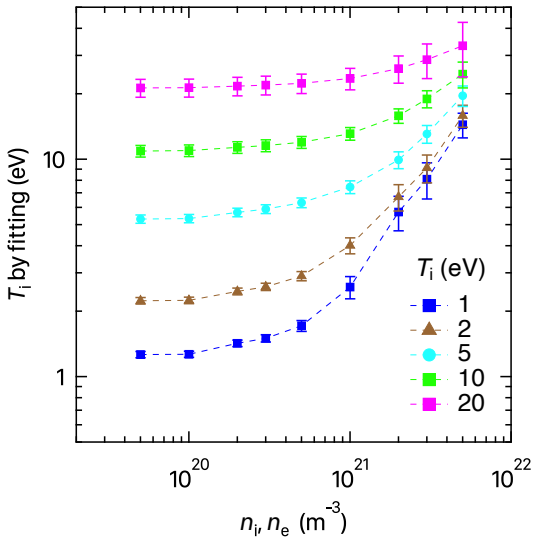

FIG. 3. Density dependence of T_i derived via fitting of calculated spectrum with a single Gaussian function.

increases with the density especially in the range where the density is higher than $10^{21}\,\mathrm{m}^{-3}$. This is considered to be an effect of the Stark broadening. The error is evaluated as the root mean square of the difference between the measured and the fitted data. It is also seen that the obtained temperature error increases with increasing density because the shape of the emission lines is no longer well represented by a single Gaussian. It should be noted that even when the density is lower than $10^{20}\,\mathrm{m}^{-3}$, T_i obtained by fitting is higher than the assumed temperature value. This is caused by the splittings of emission line components due to the Zeeman effect. In summary, we have studied the Stark broadening in a magnetic field for a beryllium ion emission line. When the electron density exceeds $10^{21}\,\mathrm{m}^{-3}$, which is a possible condition in the ITER divertor plasma, it has been confirmed that the Stark broadening becomes significant so that the ion temperature measurement can be affected.

4. RESULTS AND DISCUSSION FOR BORON ION LINES

Up to this point, the discussion has focused on the emission lines of singly ionized beryllium, but since the adoption of beryllium in ITER is expected to be avoided, it is necessary to consider the use of emission lines from other ions. As another impurity that can be used in divertor diagnostics, boron, which is applied for wall conditioning, can be considered. Here, we investigate singly ionized boron ions as a possible alternative to singly ionized beryllium ions.

The singly ionized beryllium ion is lithium-like, and except for $L = 0$, each term has two fine structures. Here, L denotes the orbital angular momentum quantum number. As a result, the Zeeman effect is anomalous, and the spectrum can have a complex structure, which, as mentioned above, affects the observed line broadening. On the other hand, the singly ionized boron ion is beryllium-like, and its energy levels are divided into singlets or triplets. In general, emission lines accompanied by transitions among triplet energy levels have higher intensity compared to those of singlets, making them advantageous for diagnostics. However, the line splitting due to the Zeeman effect may have an even more complex structure than in the case of doublets.

For the BII $(1\mathrm{s}^2 2\mathrm{s})\,3\mathrm{d}\,{}^3\mathrm{D}$ – $4\mathrm{f}\,{}^3\mathrm{F}$ (412 nm) transition, the emission line profile was calculated in the same manner as before. Since the values for the impact approximation are not given in Ref. [9], we used the PPP code [?] for the calculation. The result for $B = 5\,\mathrm{T}$, $n_\mathrm{i} = n_\mathrm{e} = 10^{21}\,\mathrm{m}^{-3}$, and ion temperature of 1 eV is shown in Fig. 4. The line profile shows a complicated structure due to the anomalous Zeeman effect, indicating that ion temperature diagnostics is difficult.

Although the emission lines of singlets are expected to be weaker in relative intensity, the Zeeman effect is strictly normal, and the structure should be simpler than that of triplet emission lines. The calculation was carried out for the BII $(1\mathrm{s}^2 2s)\,3\mathrm{d}\,{}^1\mathrm{D}$–$4\mathrm{f}\,{}^1\mathrm{F}$ (494 nm) transition. Again, Stark broadening under the impact approximation was obtained using the PPP code. The results under $B = 5\,\mathrm{T}$ for several values of n_i and n_e are shown by black solid lines in Fig. 5. The emission line splits into three components due to the normal Zeeman effect. The central peak corresponds to the π component, while the two side peaks correspond to the σ components. Since the line of sight has an angle of 60 degrees with respect to the magnetic field, the σ to π intensity ratio does not become $1/2$.

Focusing on the line profile, at $n = 2 \times 10^{20}\,\mathrm{m}^{-3}$ almost no broadening is observed, but as density increases, significant broadening is seen. Similar to the case of beryllium ions, the convolution integral of this result with the Doppler broadening at 1 eV is shown as plus symbols, and the fit using the superposition of three Gaussian functions is shown as red solid lines. The ion temperature was evaluated from the line width obtained by the fitting, and the results are shown as blue squares in Fig. 5. When the density exceeds $5 \times 10^{20}\,\mathrm{m}^{-3}$, a deviation from the assumed 1 eV appears, and the difference grows larger. This is the effect of Stark broadening. The same analysis was carried out for various assumed temperatures, and the results are also shown in Fig. 5. It can be seen that at higher temperatures, Doppler broadening becomes dominant and the effect of Stark broadening becomes less visible.

For singly ionized boron ions, it is empirically known that the emission line BII $(1\mathrm{s}^2)\,2\mathrm{s}2\mathrm{p}\,{}^1\mathrm{P}$–$2\mathrm{p}^2\,{}^1\mathrm{D}$ (345 nm), whose upper level is a doubly excited state, has relatively high intensity. Since the upper level of this emission line is optically allowed and has no nearby energy levels, the effect of Stark broadening is considered small. Indeed, when the emission line broadening was calculated using the same method as before, it was found that in the present range of electron densities, Stark broadening can be neglected. The results are overplotted with triangles in Fig. 5. By using these results together, i.e., deriving the ion temperature from the 345 nm emission and then deriving the electron density from the 494 nm emission, simultaneous diagnostics of ion temperature and electron density

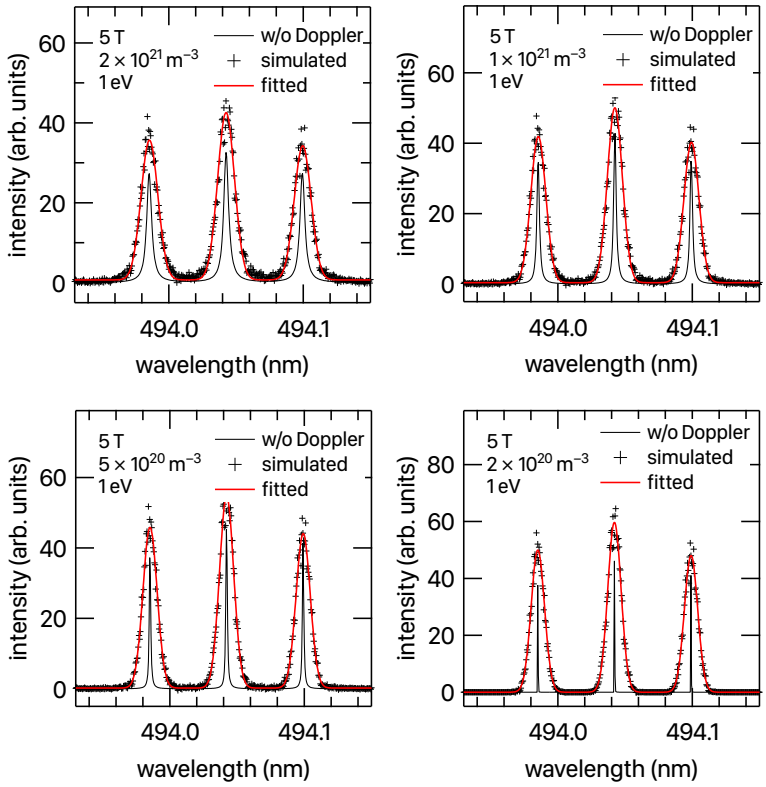

FIG. 4. Examples of calculated spectra of the Be II line $(1s^2 2s)\ 3d\ ^3D - 4f\ ^3F$ (412 nm) for four different perturber density cases when $T_i = 1$ eV.

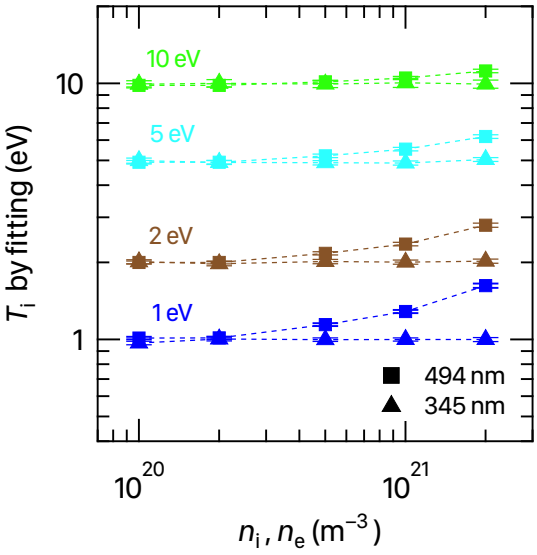

FIG. 5. Density dependence of T_i derived via fitting of calculated spectrum with three Gaussian function.

becomes possible.

In the above discussion, instrumental broadening of the spectrometer has not been considered. In actual measurements, the spectrometer dispersion must be set so that the Doppler broadening and Stark broadening of interest can be measured with sufficient accuracy. Instrumental broadening must also be taken into account when evaluating the measurable parameter range.

5. SUMMARY

With ITER divertor diagnostics in mind, the effect of Stark broadening on ion temperature measurements was evaluated for the emission lines of singly ionized beryllium ions. It was found that in density regions exceeding $10^{21}\,\mathrm{m}^{-3}$, the effect of Stark broadening becomes significant. Since the use of beryllium in ITER is expected to be avoided, the application of boron ions, used in wall conditioning, for ion temperature diagnostics was investigated. Among the two emission lines at 494 nm and 345 nm, the 494 nm line exhibits Stark broadening effects at densities higher than $5 \times 10^{20}\,\mathrm{m}^{-3}$, while the 345 nm line is hardly affected in the observed profile. These results indicate the possibility of simultaneous diagnostics of ion temperature and electron density using the two emission lines.

ACKNOWLEDGEMENTS

This work was performed partially under the support of the NIFS Collaboration Research Program (NIFS22KIEH003). M.G. thanks Nader Sadeghi for discussions on the calculation method.

REFERENCES

REFERENCES

[1] KAVEEVA, E. et al., SOLPS-ITER modeling of deuterium throughput impact on the ITER SOL plasma. Nucl. Mater. Energy 35 (2023) 101424.

[2] PITTS, R. A. et al., Physics basis for the first ITER tungsten divertor, Nucl Mater Energy 20 (2019) 100696.

[3] SADEGHI, N. and GOTO, M., Doppler-free, laser saturated absorption profile of 414 nm helium line for plasma density measurements, J. Quant. Spectrosc. Radiat. Transf. 245 (2020) 106875.

[4] HOOPER, C. F., Asymptotic Electric Microfield Distributions in Low-Frequency Component Plasmas, Phys. Rev. 169 (1968) 193–195.

[5] HOOPER C. F., Low-Frequency Component Electric Microfield Distributions in Plasmas, Phys Rev 165 (1968) 215—222.

[6] FUJIMOTO, T. and IWAMAE, A., Plasma Polarization Spectroscopy, Springer, Berlin, 2008.

[7] SAKUKRAI, J. J., Modern Quantum Mechanics, 1985.

[8] HECKMANN, P. H. and TRAEBERT, Introduction to the Spectroscopy of Atoms, North-Holland Personal Library, 1989.

[9] GRIEM, H. Spectral Line Broadening by Plasmas, ACADEMIC PRESS, INC, 1974.

[10] CALISTI et al., Fast numerical methods for line shape studies in hot and dense plasmas, J. Quant. Spectrosc. Radiat. Transf. 51 (1994) 59–64.